

# 6-Meter Beam Waveguide Antenna for Ground Based Terahertz Telescope

Vijay K. Singh, Yogesh Tyagi\*, Pratik Mevada,  
Soumyabrata B. Chakrabarty, and Milind B. Mahajan

**Abstract**—This paper discusses the design of a 6-m Cassegrain optics based multiband reflector antenna integrated with beam waveguide (BWG) optics, which consists of an ellipsoidal mirror and three plane mirrors. The presented antenna has been simulated, and 75.8% and 76.8% aperture efficiencies have been achieved at 0.225 THz and 0.338 THz, respectively. The initial design parameters of elements of BWG network are computed using fundamental Gaussian beam parameters. The simulated results of the antenna including aperture efficiency have been presented and discussed in detail. The antenna has been designed for the ground based THz telescope for radio astronomy.

## 1. INTRODUCTION

Radio astronomy is an evolving field of research and performed using ground based and space based terahertz (THz) telescope [1–5]. At millimeter and submillimeter (mm and sub-mm) frequencies it can be used in radiometric information content analysis for planet atmospheric constituents [16]. Usually, ground based astronomical radio telescopes are designed using multiband large segmented reflector antennas [6, 7]. At THz frequency, the signal received from large dish antenna is guided in free space using beam waveguide (BWG) optics [2, 8–10] and collected by feed that is followed by cryocooled low noise receiver front end. At frequencies higher than approximately 700 GHz superconductor-insulator-superconductor (SIS) technology based receiver is used [17]. BWG optics provided minimal transmission losses in comparison to metallic hollow waveguide and are generally designed using flat and curved mirrors.

The design of BWG optics is initiated by Gaussian beam technique that is based on Gaussian beam approximation of the electromagnetic (EM) fields [8, 11, 12]. The main controlling parameters of the Gaussian beam are beam radius, radius of curvature of phase front, and focal length of mirror equivalent lenses. The initial design dimensions of the mirror are decided using these parameters, for minimum spillover losses. After the initial design of the BWG optics, the accurate analysis using physical optics (PO) based technique is carried out using commercial software tool TICRA GRASP. The design of the feed horn is carried out using tools like CHAMP (mode-matching based technique) and HFSS (finite element based technique).

In this paper, the design of a 6-m dual-band BWG fed Cassegrain reflector antenna is presented. Multiflare angle horn [13] has been used as the high performance feed horn. Multiflare angle horn provides excellent RF performance, similar to the corrugated horn, for a moderate bandwidth, and it is easier to fabricate than spline and corrugated horn. Two feed horns are designed such that the radiation pattern performance remains close to a fundamental Gaussian beam having symmetric pattern and low side lobe levels (SLL). The paper is organized in four sections, which describe BWG antenna optics, its equivalent geometry, design details, and simulation results.

---

*Received 26 May 2021, Accepted 1 September 2021, Scheduled 21 September 2021*

\* Corresponding author: Yogesh Tyagi (tyagi@sac.isro.gov.in).

The authors are with the Space Applications Centre (SAC), Indian Space Research Organisation (ISRO), Ahmedabad, India.

## 2. BEAM WAVEGUIDE ANTENNA OPTICS

Figure 1 shows the schematic of a 6-m cassegrain optics based reflector antenna and BWG optics based network having multiple mirrors. The BWG optics network consists of an ellipsoidal mirror M1 and three plane mirrors (PM1, PM2, and PM3). These components effectively fold and guide the launched EM beam, towards the hyperboloidal mirror M3, which subsequently illuminates the paraboloidal main reflector M4.

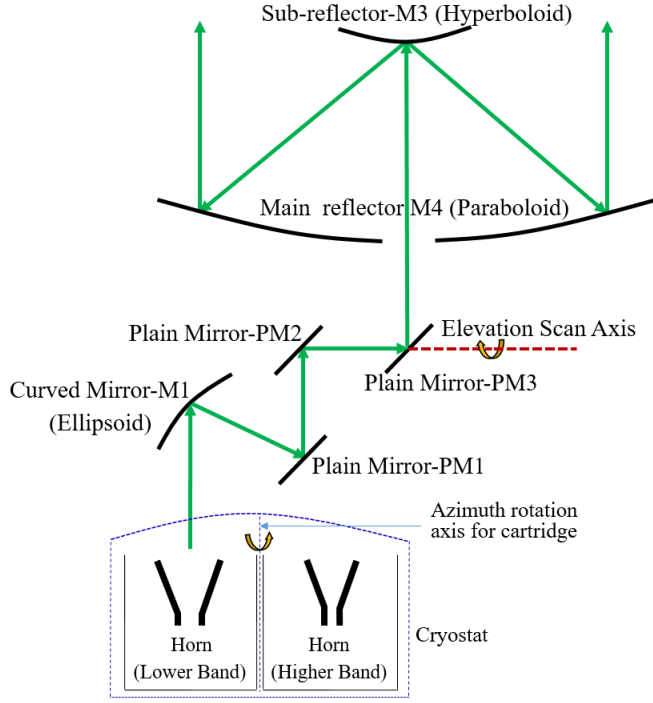


**Figure 1.** Schematic of shaped Cassegrain beam waveguide antenna for 6-m terahertz telescope.

As shown in Fig. 1, the feed horns at both bands are kept in a cooled cartridge. Moreover, for the astronomical observation, the elements of BWG optics network are rotated in azimuth, and PM3, M3, and M4 are rotated in elevation. Once the astronomical observation is completed with the lower band feed, the cartridge is rotated in azimuth by  $180^\circ$ , which brings higher band feed on the focus of ellipsoidal mirror M1. To enable elevation scanning, the presented BWG optics includes two more plane mirrors, as opposed to the optics presented in [15], for a 3 m unshaped antenna.

The antenna size is based on the required maximum gain and can be calculated using following equation.

$$\text{Gain} = \eta \left( \frac{\pi D}{\lambda} \right)^2$$

Large  $F/D$  improves the cross polarization performance significantly, and it is also desirable if an off-axis feed is to be used; otherwise, the size lobe level (SLL), especially the coma lobe, rises much slower for a large  $F/D$  ratio. On the other side, the spillover depends on the  $F/D$  ratio of the paraboloid. Spillover efficiency of a short focal length antenna is larger than that with long focal length. So there is an optimal  $F/D$  ratio as far as aperture efficiency is concerned which depends on the illumination taper and comes around 0.4 for this particular geometry. Optimum value of ratio  $D_{\text{sub}}/D_{\text{main}}$  is selected to minimize the multiplication of blockage loss and diffraction loss. Antenna optical parameters are listed in Table 1.

**Table 1.** Antenna optical parameters.

Symbol	Description	Value
$D_{\text{main}}$	Main reflector diameter	6000 mm
$D_{\text{sub}}$	Subreflector diameter	522 mm
$F$	Main reflector focal length	2400 mm
$F/D_{\text{main}}$	Main reflector F/D ratio	0.4
$e$	Subreflector eccentricity	1.064
$2f$	Distance between focal points of sub reflector	3461.5 mm
$2a$	Distance between vertices points of sub reflector	3252.0 mm
$\theta_M$	Main reflector half subtended angle	64 degree
$\theta_S$	Subreflector half subtended angle	4.4 degree
$Ft$	Field taper at subreflector	-35 dB

### 3. EQUIVALENT LENS GEOMETRY OF THE BEAM WAVEGUIDE ANTENNA

The equivalent lens sequence of the presented BWG optics network is shown in Fig. 2 and used to compute Gaussian beam parameters. Here, M1 and M3 mirrors are represented as thin lenses, and PM1, PM2, and PM3 mirrors are shown using the dotted lines. The input and output beam radii are assumed equal under thin lens approximation of a mirror. Here, lenses are modeled to change the beam parameters, and flat mirrors are modeled to reflect the beam. As shown in Fig. 2, the minimum beam radius is called the beam waist ( $w$ ) of the Gaussian beam. The computation of Gaussian beam parameters, like beam radius ( $w$ ), phase front radius of curvature ( $r$ ), input radius of curvature ( $r_1$ ), and output radius of curvature ( $r_2$ ), can be carried out using Equations (4), (5), and (6) in [8]. Here, it should be noted that the output beam parameters ( $r_2, w_2$ ) are the functions of the input beam parameters ( $r_1, w_1$ ), wavelength ( $\lambda$ ), and the distance traveled by the Gaussian beam.

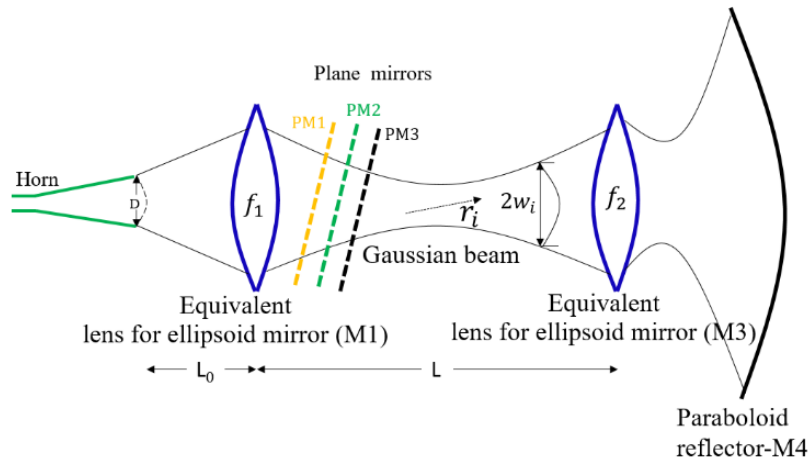


**Figure 2.** Equivalent lens geometry of BWG antenna.

If the beam’s input phase front radius of curvature and focal length of a lens are known, the output phase front radius of curvature can be computed [5] from following equation

$$\frac{1}{f} = \frac{1}{r_1} + \frac{1}{r_2} \tag{1}$$

If ( $r_1, w_1$ ) of the first lens and the length ‘ $L$ ’ between the two lenses is known, the parameters ( $r_2, w_2$ )

at the second lens can be computed [5] from Equations (2) and (3) as follows.

$$w_2 = w_1 \sqrt{\left(-\frac{L}{r_1} - 1\right)^2 + \left(\frac{\lambda L}{\pi w_1^2}\right)^2} \quad (2)$$

$$r_2 = L / \left[ 1 + \frac{\left(-\frac{L}{r_1} - 1\right)}{\left(-\frac{L}{r_1} - 1\right)^2 + \left(\frac{\lambda L}{\pi w_1^2}\right)^2} \right] \quad (3)$$

#### 4. DESIGNING OF THE BEAM WAVEGUIDE ANTENNA

Antenna designing has been carried out at two THz frequency bands, i.e., 0.218–0.232 THz (lower band) and 0.328–0.348 THz (higher band). The design has been carried out by incorporating the RF as well as mechanical constraints. One of the critical mechanical constraints is to place and space the BWG optics such that the main reflector with its back up support structure does not interfere with the cartridge and BWG mirrors, when the main reflector points towards horizon during the elevation scanning. Another constraint is to accommodate BWG mirrors in a compact volume, while maintaining the low spillover loss and any hindrance free field of view. Moreover, the minimum distance limit between the main reflector vertex and the plane mirror PM3 is set to 1700 mm due to the mechanical constraints. Here, the size of the curved and flat mirrors of BWG networks is minimized by the controlling the beam divergence and beam radius.

The feed horns are designed, yielding the Gaussian beam having high gain ( $> 25$  dBi), symmetric radiation pattern, and low SLL. At the feed aperture, the Gaussian beam diameter ( $2w$ ) and radius of curvature ( $r$ ) are 7.1 mm and 40.65 mm, respectively, at 0.225 THz (lower band). Those are 4.5 mm and 25.75 mm, respectively, at 0.338 THz (higher band). The relationship of the Gaussian beam radius of a horn and its aperture radius is broadly elaborated in [14].

The focal length of the ellipsoidal mirror is opted such that the propagation beam does not diverge, which effectively leads to the minimum size of flat mirrors and sub-reflector. The computation of beam radius is carried out at the location of each mirror of BWG network. Initially, the radius of each mirror is kept twice the computed beam radius to have amplitude taper  $< -34$  dB at the edge of each mirror and spillover efficiency close to 100% for each mirror. By taking the feed horn beam parameters as reference, the Gaussian beam parameters at input and output are evaluated for all other mirrors. The computed Gaussian beam parameters for the elements of BWG network are listed in Table 2. Here, the main reflector  $F/D$  is fixed to 0.4.

The optimized sizes of ellipsoid, PM1, PM2, and PM3 are 216 mm, 162 mm, 126 mm, and 108 mm, respectively. The distance from PM3 to the vertex of the main reflector is 1700 mm. The distance from main reflector vertex to sub-reflector is 2295 mm. The beam travels a distance of 4682 mm from the ellipsoid M1 to the sub-reflector M3. The distance from lower band feed horn to M1 is 316 mm. The focal lengths of M1 and M3 are 268 mm and  $-108$  mm, respectively. The diameter of the sub-reflector is 522 mm.

#### 5. SIMULATION RESULTS

The 6-m Cassegrain optics based reflector antenna with BWG network has been modeled using QUASt module of Tlcra GRASP-10.6. The BWG mirrors have been adjusted as per the computed parameters in Table 2. The QUASt equivalent model was simulated using PO based solver of Tlcra GRASP 10.6. The simulation was carried out at the center frequency of the lower band. The simulation results showed the desirable aperture efficiency at lower band, but poor gain at the higher band. This was attributed to the reduced beam radius at the sub-reflector at higher band. The gain performance at higher band has been improved by optimizing the feed distance from M1.

The smooth wall compound profile horns of circular aperture have been designed and simulated for both frequency bands and offered the desired Gaussian beam performance. To match the standard

**Table 2.** Gaussian beam parameters (GBP) for BWG elements.

S. No.	parameters	Lower band center	Higher Band center
1.0	GBP at <i>i/p</i> and <i>o/p</i> of Ellipsoid Mirror — M1 (in mm)		
	$r_1(i/p)$	331.3	324.8
	$w_1(i/p) = w_2(o/p)$	49.0	49.7
	$r_2(o/p)$	1403.5	1531.9
2.0	GBP at <i>i/p</i> and <i>o/p</i> of Plane Mirror — PM1 (in mm)		
	$w_1(i/p) = w_2(o/p)$	38.98	40.23
	$r_1(i/p) = r_2(o/p)$	1137.0	1062.0
3.0	GBP at <i>i/p</i> and <i>o/p</i> of Plane Mirror — PM2 (in mm)		
	$w_1(i/p) = w_2(o/p)$	30.73	31.03
	$r_1(i/p) = r_2(o/p)$	925.6	828.7
4.0	GBP at <i>i/p</i> and <i>o/p</i> of Plane Mirror — PM3 (in mm)		
	$w_1(i/p) = w_2(o/p)$	25.83	25.45
	$r_1(i/p) = r_2(o/p)$	807.6	689.7
5.0	GBPs at <i>i/p</i> and <i>o/p</i> of Hyperboloid Mirror — M2 (in mm)		
	$r_1(i/p)$	3392.0	3217.0
	$w_1(i/p) = w_2(o/p)$	121.4	105.6
	$r_2(o/p)$	-104.7	-104.5
6.0	Beam waist size after ellipse	11.8	7.33
7.0	Distance of beam waist from PM3	638.27	805.30
8.0	$w$ at reflector vertex	40.05	41.92
9.0	GBP at <i>i/p</i> and <i>o/p</i> of Hyperboloid Mirror — M2 at 0.338 THz for feed at 326 mm		
	$r_1(i/p)$		3377.0 mm
	$w_1(i/p)$		129.9 mm
	$r_2(o/p)$		-104.7

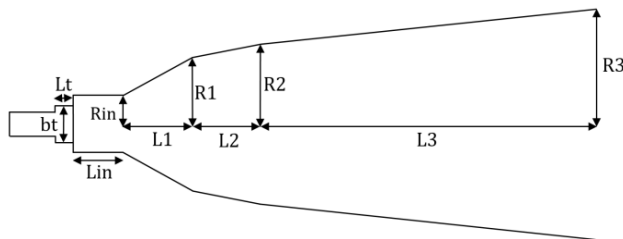


**Figure 3.** Schematic of the multiflare angle horn antenna with circular to rectangular standard waveguide transition.

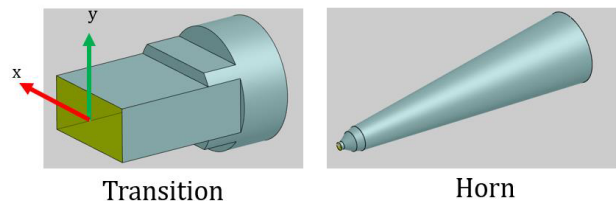


**Figure 4.** Electromagnetic analysis model of multiflare horn and input transition.

rectangular waveguide interfaces at both the bands, circular to rectangular waveguide transitions have been designed. Here, WR-4.3 and WR-2.8 standard waveguide interfaces have been used. Designed horn structures have been integrated with the respective transitions and simulated and optimized using Ansys Electronics Desktop 2019 for the return loss and radiation pattern performance. Fig. 3 shows the schematic of multiflare angle horn antenna with circular to rectangular standard waveguide. Fig. 4 displays the electromagnetic analysis model of multiflare horn and its input transition. Figs. 5 and 6

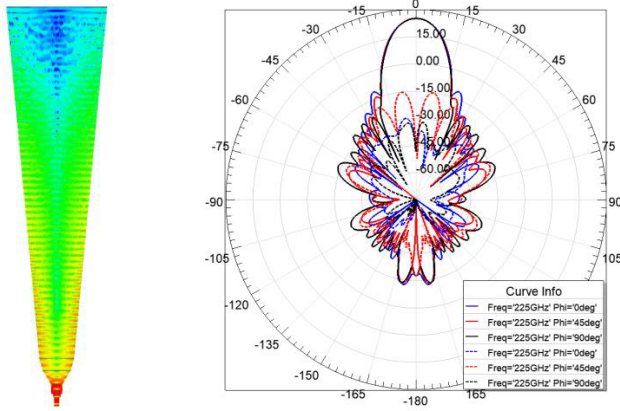


**Figure 5.** Lower band feed horn surface current distribution and radiation pattern at 0.225 THz.

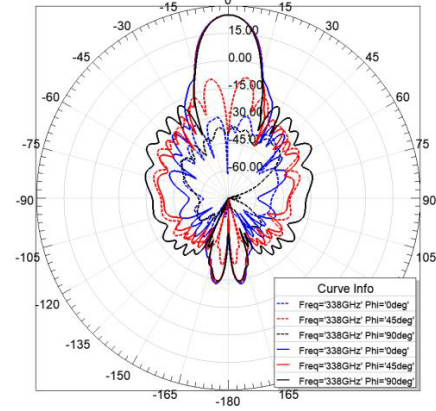


**Figure 6.** Lower band feed horn radiation pattern at 0.338 THz.

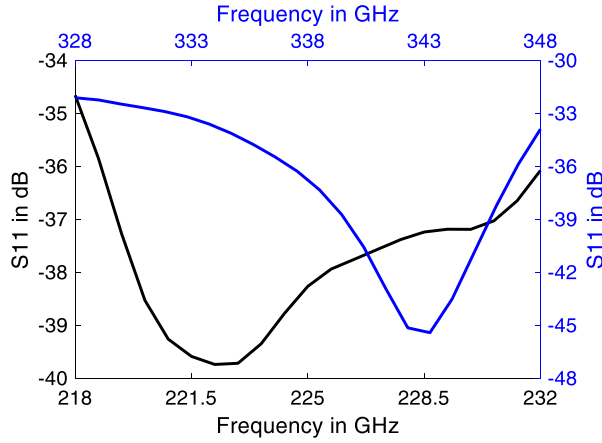


**Figure 7.** Return loss performance of lower band (black) and higher band (blue) feed horns over the frequency band.

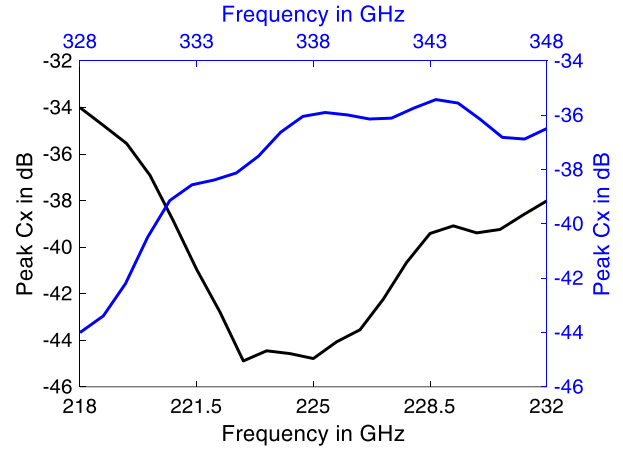


**Figure 8.** Peak cross polarization of lower band (black) and higher band (blue) feed horns over the frequency band.

**Table 3.** Simulated RF performance of feed horns.

Sr. No.	Parameters	(0.218–0.232) THz	(0.328–0.348) THz
1.	Aperture Efficiency (%)	$75.8 \pm 4.0$	$76.8 \pm 4.0$
2.	Beam Efficiency (%)	$84.4 \pm 5.0$	$85.9 \pm 4.0$
3.	Gain (dBi)	$81.8 \pm 0.2$	$85.4 \pm 0.2$
4.	Cross-pol Level (dB)	$27.9 \pm 1.0$	$28.1 \pm 1.0$
5.	Side Lobe Level (dB)	$23.4 \pm 0.5$	$22.5 \pm 0.5$
6.	HPBW (millidegree)	$14.7 \pm 0.1$	$9.84 \pm 0.1$

show the simulated radiation patterns of multiflare angle horns at 0.225 THz and 0.338 THz, respectively. Figs. 7 and 8 exhibit the simulated return loss and peak crosspolarization performances of both feed horns over the frequency bands, respectively. The simulated RF performance of the feed horns is also summarized in Table 3.

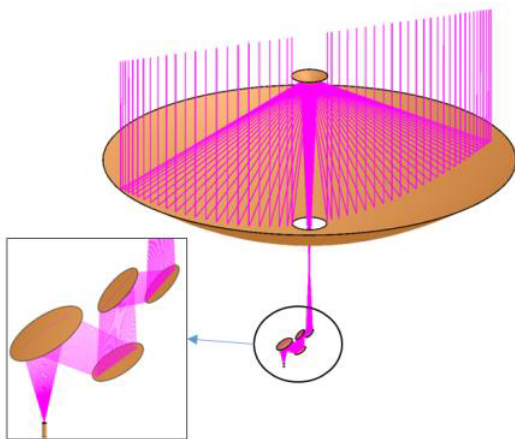


**Figure 9.** Electromagnetic analysis model of 6 m antenna system.

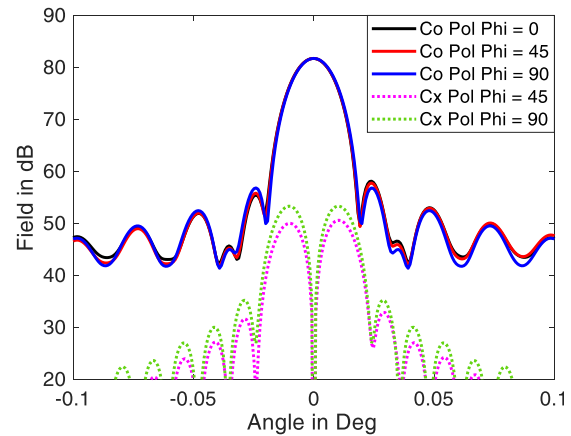


**Figure 10.** Radiation pattern of 6-m antenna at lower band (0.225 THz).

**Table 4.** Simulated performance parameters of 6-m antenna.

Sr. No.	Parameters	(0.218–0.232) THz	(0.328–0.348) THz
1.	Gain (dBi)	$(25.0 \pm 0.5)$	$(25.0 \pm 0.5)$
2.	Cross-pol Level (dB)	$< -34$	$< -35$
3.	Return Loss (dB)	$> 34$	$> 32$

The secondary analysis of the 6 m Cassegrain optics based antenna with BWG network has been repeated using the simulated primary radiation patterns of feed horns integrated with input transitions. Electromagnetic analysis model of complete antenna system is presented in Fig. 9.

Figures 10 and 11 display the simulated radiation pattern of 6-m antenna at 0.225 THz and 0.338 THz, respectively. Table 4 lists the simulated performance parameters at both frequency bands. The obtained aperture efficiencies are 75.8% and 76.8% at 0.225 THz and 0.338 THz, respectively.

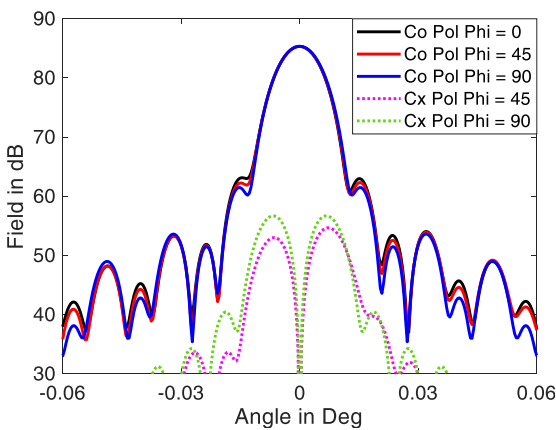


**Figure 11.** Radiation pattern of 6-m antenna at higher band (0.338 THz).

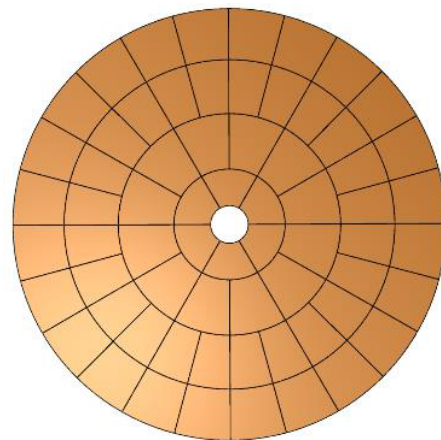


**Figure 12.** Reflector panel configuration.

## 6. FABRICATION AND REALIZATION ASPECTS 6-M ANTENNA

In order to meet the required aperture efficiency, the losses due to surface RMS and misalignments should be minimized, especially at higher frequency band. Here, the overall surface RMS of 6-m reflector surface should be  $\sim 30$  microns at the higher frequency band. That for the elements of BWG network should be  $< 5$  microns. Such a stringent RMS requirement is extremely difficult to meet during the fabrication of reflector using a single metal block or composite material. Hence, it is required to segment the reflector surface, assemble and precisely align to achieve the desired surface RMS.

Therefore, a segmentation approach has been applied, and the 6 m antenna surface will be realized using 66 panels arranged in four rings as shown in Fig. 12. The innermost ring-1 consists of six panels; ring-2 consists of 12 panels; ring-3 consists of 24 panels; and the outermost ring-4 consists of 24 panels. In order to achieve overall surface rms of better than 30 microns in 6 m antenna, each panel should be fabricated with better than 10–12 micron surface rms. The contribution of panel misalignment to total surface rms will be around 15 microns. Peak gain loss due to 30 micron surface rms is 0.29 dB and 0.68 dB at 0.225 THz and 0.388 THz, respectively.

## 7. CONCLUSIONS

In this paper, the configuration, design, and simulated performance of a 6 m Cassegrain optics based multiband reflector antenna with a BWG network is discussed in detail. The operating frequency bands for the proposed antenna are 0.218–0.232 THz and 0.328–0.348 THz. The BWG network is designed using three plane mirrors and one ellipsoidal mirror, to obtain the required illumination on the main reflector at both frequency bands. Two multiflare angle horns, along with the transitions have also been designed, achieved good pattern symmetry, and simulated using Ansys HFSS. The initial analysis of the reflector geometry has been carried out using the QUASt module of TICRA GRASP-10.6, followed by the PO analysis of the same with the simulated radiation patterns of the feed horns. The analyzed performance of the reflector antenna showed 75.8% and 76.8% aperture efficiencies at 0.225 THz and 0.338 THz, respectively. The proposed THz band reflector antenna is to be utilized as a radio telescope for astronomical observations of molecular clouds. The development of the antenna is to be carried out with high accuracies to meet the required specifications. Therefore, the surface RMS related discussion has also been included, and it has been recommended that the reflector surface development should be carried out using the segmentation technique.

## ACKNOWLEDGMENT

The authors would like to thank and appreciate the support of Shri. N. M. Desai, Director, SAC to carry out this work. The authors also wish to thank the Scientists and Engineers of Microwave Sensor Antenna Division (MSAD) for their support.

## REFERENCES

1. Stacey, G. J., “New ground based facilities for THz astronom,” *19th International Symposium on Space Terahertz Technology*, 33–41, Groningen, April 28–30, 2008.
2. Onishi, T., A. Nishimura, Y. Ota, A. Hashizume, Y. Kojima, A. Minami, K. Tokuda, S. Touga, Y. Abe, M. Kaiden, K. Kiimura, K. Muraoka, H. Maezawa, H. Ogawa, K. Dobashi, T. Shmoikura, Y. Yonekura, S. Asayama, T. Handa, T. Nakajima, T. Noguchi, and N. Kuno, “A 1.85-m mm-submm telescope for large-scale molecular gas surveys in  $^{12}\text{CO}$ ,  $^{13}\text{CO}$ , and  $\text{C}^{18}\text{O}$  ( $J = 2 - 1$ ),” *Astron. Soc. Japan*, Vol. 65, No. 78, 61–64, August 2013.
3. Yang, J., Y.-X. Zuo, Z. Lou, J.-Q. Cheng, Q.-Z. Zhang, S.-C. Shi, J.-S. Huang, Q.-J. Yao, and Z. Wang, “Conceptual design studies of the 5 m terahertz antenna for Dome A, Antarctica,” *Research in Astro. Astrophys.*, Vol. 13, No. 12, 1493–1508, 2013.
4. Sørensen, S. B. and K. Pontoppidan, “Analysis of the ALMA telescope and front-ends,” *21st International Symposium on Space Terahertz Technology*, 121–127, Oxford, March 23–25, 2010.

5. Rolo, L. F., M. H. Paquay, R. J. Daddato, J. A. Parian, D. Doyle, and P. de Maagt, "Terahertz antenna technology and verification: Herschel and Planck — A review," *IEEE Transactions on Microwave Theory and Techniques*, Vol. 58, No. 7, 2046–2063, July 2010.
6. Wang, C., H. Li, K. Ying, Q. Xu, N. Wang, B. Duan, W. Gao, L. Xiao, and Y. Duan, "Active surface compensation for large radio telescope antennas," *Hindawi Int. J. of Antenna and Propagation*, 1–17, Article ID 3903412, 2018.
7. Navarrini, A., et al., "Front-ends and phased array feeds for the sardinia radio telescope," *32nd URSI GASS*, Montreal, August 19–26, 2017.
8. Chu, T.-S., "An imaging beam waveguide feed," *IEEE Transactions on Antennas and Propagation*, Vol. 31, No. 4, 614–619, July 1983.
9. Paine, S., D. C. Papa, R. L. Leombruno, X. Zhang, and R. Blundell, "Beam waveguide and receiver optics for the SMA," *Fifth International Symposium on Space Terahertz Technology*, 811–823, Michigan University, May 1994.
10. Sugimoto, M., M. Carter, J. Inatani, Y. Sekimoto, and S. Iguchi, "Design of corrective beam waveguide system for the ALMA/ACA 7-m antenna," *Pub. Astro. Soc. Japan*, Vol. 61, 1065–1080, October 25, 2009.
11. McEwan, N. J. and P. F. Goldsmith, "Gaussian beam techniques for illuminating reflector antennas," *IEEE Transactions on Microwave Antennas and Propagation*, Vol. 37, No. 3, 297–304, March 1989.
12. Whale, M., "Optical characterisation of astronomical submillimetre receivers including ALMA bands 5 and 9," A Ph. D thesis, NUI Maynooth, Maynooth, Co. Kildare, Ireland, January 2010.
13. Chahat, N., T. J. Reck, C. Jung-Kubiak, T. Nguyen, R. Sauleau, and G. Chattopadhyay, "1.9-THz multiflare angle horn optimization for space instruments," *IEEE Transactions on Terahertz Science and Technology*, Vol. 5, No. 6, November 2015.
14. Wylde, R. J. and D. H. Martin, "Gaussian beam-mode analysis and phase-centers of corrugated feed horns," *IEEE Transactions on Microwave Theory and Techniques*, Vol. 41, No. 10, 1691–1699, October 1993.
15. Singh, V. K., Y. Tyagi, S. Rakshit, A. Solanki, B. K. Pandey, S. B. Chakrabarty, and M. B. Mahajan, "Dual-band beam waveguide fed terahertz antenna for ground telescope," *CAP-2019*, Ahmedabad, December 19–22, 2019.
16. Mathew, N., S. Sahoo, R. Ramachandran Pillai, and C. Suresh Raju, "Millimeter-wave radiometric information content analysis for venus atmospheric constituents," *Special Issue of the 2019 URSI Asia-Pacific Radio Science Conference*, 2019.
17. Uzawa, Y., Y. Fujii, T. Kojima, M. Kroug, W. Shan, S. Ezaki, A. Miyachi, H. Kiuchi, and A. Gonzalez, "Superconducting receiver technologies supporting ALMA and future prospects," *Special Issue of the 2019 URSI-Japan Radio Science*, 2019.